Neuroligins Facilitate The Development of Bone Cancer Pain via Regulating Synaptic Transmission

Xianqiao Xie
Department of Anesthesiology, Suizhou Central Hospital, Suizhou

Yang Li
Institute of Anesthesiology & Pain (IAP), Department of Anesthesiology, Taihe Hospital, Hubei University of Medicine, Shiyan, Hubei

Shanchun Su
Institute of Anesthesiology & Pain (IAP), Department of Anesthesiology, Taihe Hospital, Hubei University of Medicine, Shiyan, Hubei

Xiaohui Li
Institute of Anesthesiology & Pain (IAP), Department of Anesthesiology, Taihe Hospital, Hubei University of Medicine, Shiyan, Hubei

Xueqin Xu
Institute of Anesthesiology & Pain (IAP), Department of Anesthesiology, Taihe Hospital, Hubei University of Medicine, Shiyan, Hubei

Dongsheng Sun
Institute of Anesthesiology & Pain (IAP), Department of Anesthesiology, Taihe Hospital, Hubei University of Medicine, Shiyan, Hubei

Yan Gao
Department of Nuclear Medicine and Institute of Anesthesiology & Pain (IAP), Taihe Hospital, Hubei University of Medicine, Shiyan, Hubei

Minjing Peng
Institute of Anesthesiology & Pain (IAP), Department of Anesthesiology, Taihe Hospital, Hubei University of Medicine, Shiyan, Hubei

Yanqiong Wu
Institute of Anesthesiology & Pain (IAP), Department of Anesthesiology, Taihe Hospital, Hubei University of Medicine, Shiyan, Hubei

Changbin Ke (changbinke-iap@taihehospital.com)
Institute of Anesthesiology & Pain (IAP), Department of Anesthesiology, Taihe Hospital, Hubei University of Medicine, Shiyan, Hubei

---

Research Article

Keywords: bone cancer, chronic pain, neuroligins, synaptic transmission, GABAergic, glutamatergic

Posted Date: November 9th, 2021

DOI: https://doi.org/10.21203/rs.3.rs-991135/v1

Abstract

Background

The underlying mechanism of chronic pain involves the plasticity in synaptic receptors and neurotransmitters. This study aimed to investigate potential roles of neuroligins (NLs) within the spinal dorsal horn of rats in a newly established bone cancer pain (BCP) model.

Methods

Using our rat BCP model, we assessed pain hypersensitivity over time. Quantitative real-time polymerase chain reaction and Western blot analysis were performed to investigate NL expression, and NLs were overexpressed in the rat spinal cord using lentiviral vectors. Immunofluorescence staining and whole-cell patch-clamp recordings were deployed to investigate the role of NLs in the development of BCP.

Results

We observed reduced expression levels of NL1 and NL2, but not NL3, within the rat spinal cord, which were found to be associated with and essential for the development of BCP in our model. Accordingly, NL1 or NL2 overexpression in the spinal cord alleviated mechanical hypersensitivity of rats. Electrophysiological experiments indicated that NL1 and NL2 are involved in BCP via regulating γ-aminobutyric acid-ergic interneuronal synapses and the activity of glutamatergic interneuronal synapses, respectively.

Conclusions

Our observations unravel the role of NLs in cancer-related chronic pain and further suggest that inhibitory mechanisms are central features of BCP in the spinal dorsal horn. These results provide a new perspective and basis for subsequent studies elucidating the onset and progression of BCP.

1. Background

Bone cancer pain (BCP) is a major complication affecting cancer patients' quality of life substantially. Existing treatments for pain control are largely ineffective due to the poor understanding of the underlying mechanisms.

Neuroligins (NLs) are type I postsynaptic transmembrane proteins of the central nervous system that are encoded by four genes in rodents (*NL1*, *2*, *3*, and *4*) and by five in higher primates and humans (*NLGN4Y* in addition) [1]. Neurexins (NRXNs) are presynaptic transmembrane proteins associated with the release of presynaptic transmitters. The extracellular cholinesterase-homology (ChE) domain of NLs interacts

with the repeats of laminin G-like (LG) domains of NRXNs [2]. NL-NRXN complexes form through interactions via the ChE and LG domains and further establish trans-synaptic connections. Intracellularly, NLs interact with several postsynaptic density protein(PSD)-95/disks large/zonula occludens-1 domains of scaffolding proteins, which directly interact with postsynaptic receptors, ion channels, and other signaling proteins [3].

Different isoforms of NLs exhibit synapse-specific localization and functions. NL1 is localized to glutamatergic and some cholinergic synapses, whereas NL2 is found predominantly at γ-aminobutyric acid (GABA)ergic and glycinergic synapses; NL3 has been observed at both glutamatergic and GABAergic synapses. Conversely, NL4 is poorly conserved among NLs and has been detected at GABAergic synapses in the central nervous system and glycinergic synapses in the retina [4]. At glutamatergic synapses, NL1 couples to PSD-95 that assembles glutamate receptors and binds to presynaptic NRXNs to cluster glutamate [5–7]. At GABAergic synapses, NL2 couples to postsynaptic gephyrin via its intracellular cytoplasmic tail, and in turn recruits GABA receptors [8] and binds to presynaptic NRXNs to regulate the release of GABA [9]. Consistent with its localization, NL3 can modulate both glutamatergic and GABAergic postsynapses [10]. Although NL4 is reportedly restricted to inhibitory glycinergic synapses in mice [4], NL4-R704C complexes have been found to induce an excitatory synaptic phenotype in human stem cell-derived neurons [11]. Besides the studies on the localization and basal synaptic transmission of NLs in synapses, there are numerous studies that focused on how NLs participate in the pathophysiology of diseases, especially in relation to pain. The interaction between NL2 and PSD-95 may contribute to postoperative pain upon an increase in NL2 expression in the spinal dorsal horn [12, 13]. NL1 is involved in pain hypersensitivity by facilitating the synaptic incorporation of N-methyl-D-aspartate receptors (NMDARs) [14]. However, the level of expression and the role of NLs in different pain models remain controversial [5, 14].

In the present study, we show that modifications in the protein expression levels of NLs were involved in the excitation/inhibition equilibrium of the spinal dorsal horn, thus contributing to chronic pain in cancer-bearing rats. By confocal imaging and whole-cell patch-clamp recordings combined with behavioral analyses, we demonstrate that NL1 regulated dorsal horn superficial projection neurons' hyperactivity and mitigated mechanical allodynia through modulating the activity of GABAergic interneurons, and NL2 alleviated bone cancer-induced pain via decreasing the activity of glutamatergic neurons, which reduced the excitability of spinal cord interneurons.

2. Methods

2.1. Animals

All experimental procedures and protocols used in this study were approved by the Animal Use and Care Committee of Hubei University of Medicine (Hubei, China) and were conducted in accordance with the National Institutes of Health (NIH) guide for the care and use of laboratory animals and with the ethics guidelines of the International Association for the Study of Pain. Adult female Sprague-Dawley (SD) rats

weighing 180–220 g and newborn rats within 24 h were provided by the Institute of Laboratory Animal Science, Hubei University of Medicine (Hubei, China). Rats were housed at 22 ± 2°C with a 12-h light-dark cycle and free access to food and water.

2.2. Preparation of Walker 256 carcinoma cells

We injected 0.5–1 mL (3×10^7 cells/mL) of Walker 256 rat mammary gland carcinoma cells into the abdominal cavity of a female SD rat weighing 80–100 g. Cells were harvested by differential centrifugation from ascitic fluid 6–7 days later, diluted to achieve a final concentration of 10^6 cells/mL and kept on ice until surgery. For the sham group, Walker 256 cells were prepared in the same way but were boiled for 20 min prior to injection.

2.3. BCP model establishment

The rat BCP model was established by injection of Walker 256 rat mammary gland carcinoma cells into the bone marrow cavity of the right tibia of SD rats according to a previous report [15].

2.4. Lentivirus construction and microinjection

A lentiviral vector containing green fluorescent protein (gcGFP) was employed in this study to stably overexpress NL1 or NL3. To this end, the vector GV492 (Ubi-MCS-3FLAG-CBh-gcGFP-IRES-puromycin; Shanghai GeneChem Co. LTD, Shanghai, China) was recombined with the gene sequences of *NL1* (NM_053868; NL1-LV) or *NL3* (NM_134336; NL3-LV). The same vector framework, carrying gcGFP without the target gene sequences, was used as a negative lentivirus control (NC1-LV or NC3-LV). The lentiviral vector GV320 (Ubi-MCS-3FLAG-SV40-Cherry; Shanghai GeneChem Co. LTD, Shanghai, China) containing Cherry was recombined with the *NL2* gene sequence (NM_053512; NL2-LV) to stably overexpress this NL. The same vector backbone carrying Cherry only was used as negative control (NC2-LV). The viral titers of NL1-LV, NL2-LV, and NL3-LV were 1.0×10^9 TU/mL, 1.0×10^9 TU/mL, and 2.0×10^9 TU/mL, respectively. Following carcinoma implantation, the L4–L6 lumbar spinal cord was exposed carefully by laminectomy. A glass capillary (35 ± 5 mm diameter) containing a viral suspension (5 μM) was injected into the right spinal dorsal horn. The injection point was at 0.4 mm from the midline in the right dorsal horn, and the glass capillary was lowered into the parenchyma to 0.5 mm below the pia mater to reach the dorsal horn. Finally, the incision was dusted with penicillin powder and the skin was sutured.

2.5. Pain behavior assessment

Mechanical allodynia of rats was assessed by means of the paw withdrawal threshold (PWT) using a dynamic plantar esthesiometer (Ugo Basile, Stoelting, IL, USA) on days 0 (before surgery), 3, 6, 9, 12, 15, 18, and 21. The measurements were conducted from 8:30 to11:30 a.m. Rats were placed in separate transparent boxes on an elevated wire mesh platform. After 20 min of acclimation, mechanical allodynia was measured using the hind paw withdrawal response to von Frey filament stimulation. The filament (0.5 mm diameter) was placed beneath the hind paw until it touched the plantar surface of the paw and began to exert an upward force. The forces were recorded in grams when the withdrawal response was elicited, up to a maximum of 50 g. Each rat was assessed at least three times at intervals of 3 min.

2.6. Real-time polymerase chain reaction analysis

RNA isolation, cDNA synthesis, and real-time polymerase chain reaction (RT-PCR) were performed as previously described [16]. The gene names and forward (F) and reverse (R) primers are listed in Supplementary Table 1.

2.7. Protein extraction and Western blot analysis

Proteins from rat L4 to L6 lumbar spinal cord were extracted using radioimmune precipitation lysis buffer (CST, America). Total protein concentrations were assayed using a bicinchoninic acid protein assay kit (N3219; TIAN GEN, China). Samples were calibrated to 30 μg/μL with loading buffer solution and phosphate-buffered saline (PBS) and heated for 10 min at 95°C. Following sodium dodecyl sulfate-polyacrylamide gel electrophoresis, the proteins were transferred to a polyvinylidene fluoride membrane. Membranes were blocked with 5% skim milk in tris-buffered saline (TBS) containing 0.1% Tween (TBST) for 1 h at room temperature and incubated with primary antibodies at 4°C overnight. After three washes in TBST, they were incubated with horseradish peroxidase-linked secondary antibodies for 40 min at room temperature. Finally, the membranes were washed in TBST three times, processed using the ECL Plus kit and exposed to MP-ECL film.

2.8. Immunohistochemistry

For immunohistochemical (IHC) staining, rats were deeply anesthetized with 3% isoflurane and transcardially perfused with cold PBS followed by 4% paraformaldehyde (PFA). After perfusion, the lumbar (L4–L6) spinal cord was harvested, post-fixed in 4% PFA at 4°C for 2 h and cryoprotected in 30% sucrose in PBS at 4°C for 24 h. The frozen sections (15 μm) were blocked using 10% donkey serum at room temperature for 10 min and then incubated with primary antibodies diluted in blocking solution at 4°C overnight. For immunofluorescence detection, the slices were incubated with corresponding fluorescent secondary antibodies at room temperature in the dark for 1 h. Following washes with PBS, the stained sections were mounted by coverslips with 50% glycerinum. The sections were examined, and immunostaining images were obtained with the laser scanning confocal microscope Leica TCS SP8 (Leica, Wetzlar, Germany). The primary antibodies used are listed in Supplementary Table 2.

2.9. Electrophysiology

Primary neurons were cultured as described previously. Briefly, the neocortex of newborn rats was harvested from postnatal pups and cut into small pieces within 1 mm^3, papain-digested (10 min, 37°C), and then passed through a 400-μm mesh strainer. The dissociated cells were plated on poly-L-lysine (P7405; Sigma, America)-coated glass coverslips in 12-well plates (1.5×10^5 cells/well). The cultures were maintained in Dulbecco's Minimum Essential Medium (Gibco, America) supplemented with 10% fetal calf serum (Gibco). After 4–6 h, the culture medium was changed to Neurobasal A medium (10888-022; Gibco) supplemented with 2% B27 (17504044; Gibco) and 1% GlutaMAX (Gibco) and incubated at 37°C in 5% CO_2. Neurons were transfected with lentivirus and recorded on day 10.

In vitro whole-cell patch-clamp recordings in cultured primary neurons were performed at room temperature. The extracellular solution contained the following (in mM): 140 NaCl, 3 KCl, 2 $MgCl_2$, 2 $CaCl_2$, 10 glucose, and 10 4-(2-hydroxyethyl)-1-piperazine-ethanesulfonic acid (HEPES; pH 7.4, 300 mOsm). Borosilicate glass recording pipettes (resistance: 5–8 MΩ) were filled with intracellular solution, which contained the following (in mM): 135 K-gluconate, 2 $MgCl_2$, 10 HEPES, 1 ethylene glycol-bis(β-aminoethyl ether)-N,N,N′,N′-tetraacetic acid (EGTA), and 5 MgATP, Na_3GTP (pH 7.3, 290 mOsm). Data were collected using a Multiclamp 700B (Molecular Devices, Sunnyvale, CA, USA), filtered at 2 kHz and digitized at 10 kHz by a Digidata 1550A and Clampex 10.5 software (Molecular Devices). To elicit action potentials (APs), increasing amounts of depolarizing currents from 0 pA to 220 pA with 20 pA increments were used. The parameters of the first evoked AP were used for analysis. The evoked spontaneous excitatory postsynaptic currents (sEPSCs) and spontaneous inhibitory postsynaptic currents (sIPSCs) were recorded by holding a potential of −70 mV and 0 mV, respectively.

In vivo whole-cell patch-clamp recordings were made in superficial spinal dorsal horn neurons from adult rats. Briefly, rats were deeply anesthetized and transcardially perfused with 60 mL ice-cold cutting solution containing the following (in mM): 93 N-methyl-D-glucamine, 93 HCl, 2.5 KCl, 1.2 NaH_2PO_4, 30 $NaHCO_3$, 25 glucose, 20 HEPES, 5 Na-ascorbat, 3 Na-pyruvate, 2 thiourea, 10 $MgSO_4$, and 0.5 $CaCl_2$. Laminectomy was performed, and the lumbar enlargement was quickly removed to the ice-cold cutting solution with 95% O_2 and 5% CO_2. Sagittal slices (400 μm) were prepared with a Leica VT1000S vibratome. Subsequently, the slices were transferred into artificial cerebro-spinal fluid (containing, in mM: 126 NaCl, 2.5 KCl, 1.25 NaH_2PO_4, 26 $NaHCO_3$, 10 glucose, 2 $MgSO_4$, and 2 $CaCl_2$) and incubated for 30 min at room temperature. Under a dissecting microscope with transmitted illumination, the substantia gelatinosa was clearly visible as a relatively translucent band across the dorsal horn. Patch pipettes (3–5 MΩ) were filled with internal solution, which contained (in mM): 135 potassium gluconate, 0.5 $CaCl_2$, 2 $MgCl_2$, 10 EGTA, 10 HEPES, 0.5 Na_3GTP, and 5 MgATP. All experiments were performed at room temperature. The series resistance was 10–30 MΩ and was monitored during the process. Data were collected as described above. To elicit APs, increasing amounts of depolarizing currents were injected for 20 ms in a stepwise manner from −60 pA to 220 pA in 20 pA increments. The parameters of APs were determined from the first AP evoked at threshold. To identify the firing pattern, a 150-pA current was applied for 150 ms. The membrane potential was held at −70 mV for sEPSCs and 0 mV for sIPSCs. APs were analyzed using Clampfit 10.5 and spontaneous postsynaptic currents (sPSCs) were analyzed with Mini Analysis (Synaptosoft, America).

2.10. Statistical analysis

Data were analyzed using SPSS 22.0 software (IBM, Armonk, NY, USA) and results are presented as the mean ± SEM. Comparisons among groups were analyzed using one-way analysis of variance (ANOVA) and, where appropriate, followed by the Student-Newman-Keuls test. A value of $P < 0.05$ was considered to be statistically significant.

3. Results

3.1 Illumina HiSeq ™ revealed BCP-related genes in lumbar spinal cord and dorsal root ganglia of BCP rats

In order to identify altered genes that might relate to the formation and maintenance of BCP in the dorsal root ganglion (DRG) and spinal cord, we conducted high throughput sequencing (Illumina HiSeq™) experiments on rats with carcinoma tibia implantation and sham controls. The ipsilateral L4–L6 lumbar spinal cord and DRGs were harvested and the mRNA was sequenced using the Agilent 2100 Bioanalyzer platform (Agilent Technologies, Palo Alto, CA). The gene expression profiles in carcinoma rats were compared with those in sham controls. In DRGs, we identified 1274 differentially expressed genes, of which 684 were upregulated and 590 were downregulated (Fig. 1A, B). In spinal cord, we identified 2098 differentially expressed genes, of which 1632 genes were upregulated and 466 genes were downregulated (Fig. 1A, B). These genes are likely to be involved in the peripheral and central mechanisms of the development and/or maintenance of BCP. Gene Ontology (GO) is the international standard classification system of gene functions, which directly reflects the differentially expressed genes on GO terms enriched in biological processes, cell components, and molecular functions [17]. Unexpectedly, the GO analysis demonstrated that the differentially expressed genes involved in bone cancer-induced pain in spinal dorsal horn and DRGs were immune-related genes (Fig. 1C, D).

3.2 Decreased NL expression facilitates the development of BCP

Next, to investigate whether NLs were involved in the development of BCP, we used our newly established rat model; BCP was induced by injection of carcinoma cells into the tibia of animals and the PWT was measured to assess mechanical allodynia using a dynamic plantar esthesiometer. Lentiviruses were injected into the ipsilateral dorsal horn to overexpress NLs (NL-LV), and the expression of NLs in the spinal cord was examined by IHC, Western blot analysis, and RT-PCR. The results showed that NL1 was dispersedly distributed from the spinal dorsal horn to the ventral horn and was located mainly in the lamina I and II of the dorsal horn. Similarly, NL2 and NL3 were found predominantly in lamina I and II of the dorsal horn (Fig. 2A–C, Supplementary Fig. 1A–C). Quantitative analysis by RT-PCR and Western blot indicated that the expression of NLs was decreased in the carcinoma-bearing rats compared with sham controls, which was reversed by NL overexpression (Fig. 2D, E). The behavioral tests showed that carcinoma inoculation resulted in significant changes in pain behaviors on the ipsilateral paw, which were attenuated by the overexpression of NL1 or NL2, but not of NL3 (Fig. 2F). These results indicate that the diminished endogenous expression of either NL1 or NL2 induced the development of BCP.

3. 3 The cellular localization of NL1 and NL2 in spinal dorsal horn interneurons

Given the potential mechanism of NLs involved in the development of BCP, the distribution of NLs in neuronal cells was examined using triple immunofluorescence staining and analyzed by confocal

microscopy imaging. Our results revealed that NL1 was co-expressed with the glutamate receptor GluR1 on GABAergic neurons (Fig. 3A), indicating that it may contribute to the excitability of GABAergic neurons. NL2 was co-localized with GABAR-γ2 in glutamatergic neurons (vesicular glutamate transporter 2 [Glut2]), pointing towards a role in the regulation of inhibitory synaptic transmission in glutamatergic neurons (Fig. 3B). Taken together, the distinct expression of NLs in interneurons may have resulted in an imbalance of excitatory and inhibitory synaptic transmission in the spinal cord and could thus have induced the development of BCP.

3.4 Decreased expression of NL1 and/or NL2 inhibits synaptic transmission in spinal cord interneurons of BCP rats

To further investigate the role of NLs in synaptic transmission, we performed whole-cell patch-clamp recordings of acute spinal slices from sham, carcinoma, and carcinoma + NL1/2-LV or NC1/2-LV (respective negative control) rats, and the APs and sPSCs were recorded. We found that overexpression of NL2 increased the latency of the first AP and that of the AP evoked by a current of 200 pA (Fig. 4A–C), whereas NL1 overexpression decreased the threshold of the first AP and that of the AP stimulated by 200 pA (Fig. 4D and E). Both the frequency and amplitude of sEPSCs decreased significantly in spinal slices of carcinoma-bearing rats compared with those of sham counterparts, which was reversed by the overexpression of NL1 in spinal cord (Fig. 4F–H). Thus, it appears that diminished NL1 levels dominate the inhibitory neuronal excitability in the spinal cords of cancer-bearing rats via decreasing excitatory synaptic transmission on GABAergic neurons and therefore cause the development of BCP.

The frequency and amplitude of sIPSCs also decreased in carcinoma-bearing rats compared with sham controls, which could be reversed by overexpression of NL2 in spinal cord (Fig. 4I–K). This suggests that low levels of NL2 in cancer-bearing rats inhibit the inhibitory synaptic transmission of glutamatergic neurons and therefore cause an increase in their excitability. These results demonstrate that low expression of NL1 and NL2 reduced the excitatory and inhibitory synaptic transmission in BCP, respectively, which suggests that an underlying inhibitory mechanism may be a central feature of BCP in the spinal dorsal horn.

3.5 Overexpression of NL1 and/or NL2 changes electrophysiological properties of primary cultured rat cortical neurons

To further confirm the roles of NL1 and NL2 in synaptic transmission, whole-cell patch-clamp recording was used to identify electrophysiological properties of cultured neurons treated with NC-LV, NL1-LV, or NL2-LV. The results showed that neurons infected with NL1-overexpressing lentivirus exhibited a significantly higher input resistance (Fig. 5A, B), suggesting that upregulation of NL1 altered the membrane characteristics (such as permeability and integrity) of neurons. NL2 overexpression decreased the latency of the first AP, rise time, decay time, and increased the rise slope of evoked APs. Additionally, overexpression of NL2 decreased the depolarization time and increased the threshold of APs evoked by a

current of 200 pA (Fig. 5C–H). The overexpression of NL1, but not NL2, increased the amplitude of sEPSCs, whilst their frequency remained unchanged. Conversely, NL2 overexpression, but not NL1, caused a profound increase in the amplitude and frequency of sIPSCs (Fig. 5I–N). In summary, NL1 and NL2 played different roles in excitatory and inhibitory synaptic transmission.

4. Discussion

In this study, the expression patterns and functions of NL1 and NL2 were analyzed using different approaches in carcinoma-bearing and sham rats. Based on our *in vitro* and *in vivo* experiments, NL1 and NL2, but not NL3, are involved in the development and/or maintenance of BCP.

Previous studies have shown that NL1 is associated with pain. Recruitment of NL1 in the spinal dorsal horn contributes to inflammatory pain [5], and NL1 knockdown in this region alleviates pain hypersensitivity [14]. In our study, Western blot and RT-PCR analyses indicated that expression of NL1 was decreased in the spinal cord of BCP rats in comparison with sham controls. It has been demonstrated that NL1 is mainly concentrated on excitatory postsynaptic membranes where it regulates the excitatory synaptic transmission [18–20]. Co-localization of NL1 and GluR1 on excitatory synapses of inhibitory (glutamic acid decarboxylase-immunoreactive) neurons was observed in rats, suggesting that NL1 is not fully restricted to participate in the regulation of excitatory or inhibitory synaptic transmission. The expression of NL1 was decreased in the spinal cords of carcinoma-bearing rats compared with controls, and our electrophysiological analysis indicated that the frequency and amplitude of sEPSCs were significantly decreased in spinal slices. This is in line with previous studies, in which the suppression of NL1 decreased EPSCs of α-amino-3-hydroxy-5-methyl-4-isoxazole propionic acid receptors (AMPARs) and NMDARs [7, 21]. Whilst simultaneous knockdown of NL1, NL2, and NL3 mediated the most robust reduction of inhibitory terminals, exclusive inhibition of NL1 by specific shRNA knockdown reduced spine and vesicular GABA transporter (vGAT) sensitivity [22]. Therefore, in this study, the reduction in NL1 expression levels presumably decreased the excitatory potential of interneurons, especially GABAergic neurons, which resulted in a disinhibition of superficial projection neurons and an enhancement in the sensitivity of interneurons to noxious stimuli, and thus induced pain in carcinoma-bearing rats. Conversely, NL1 overexpression reversed the aforementioned phenomena and mitigated mechanical hyperalgesia in BCP rats. It has been reported that NL1 overexpression in hippocampus led to an increase in the expression of vGAT and increased excitation rather than altered inhibition [23]. Our whole-cell patch-clamp recordings demonstrated that the sEPSC amplitude was increased in cultured cortical neurons on NL1 overexpression. Based on our IHC results, it is possible that NL1 overexpression increased the excitatory potential of inhibitory interneurons, consequently enhancing the transmission of noxious stimuli information. Although the mechanisms underlying our observations remain unresolved, NL1 likely contributes to the development and maintenance of BCP.

According to previous studies, NL2 is localized at the inhibitory postsynaptic membrane regulating inhibitory synaptic transmission [24]. Knockout of NL2, but not NL1, reduces inhibitory synaptic neurotransmission in hippocampus and somatosensory cortex [25]. The frequency and amplitude of

sIPSCs as well as the expression of NL2 were decreased in carcinoma-bearing rats in our study, and using immunofluorescence we could show that NL2 was co-expressed with GABARγ2 and vGlut2. Altogether, these findings suggest that the inhibition of excitatory interneurons was weakened, which resulted in facilitated transmission of noxious stimuli to the central nervous system. Consequently, the carcinoma-bearing rats were hypersensitive to mechanical stimulation due to reduced NL2 levels in the spinal cord. However, the hyperalgesia was reversed through overexpression of NL2 using lentiviruses. Our electrophysiological results showed that the frequency and amplitude of sIPSCs were increased in acute spinal slices in response to the overexpression of NL2 in the spinal cord of BCP model rats as well as in cultured cortical neurons. The disparities between cortical neurons and spinal slices of adult rats regarding depolarization time and threshold of APs evoked by a current of 200 pA may have resulted from the different densities of neurons in each setting [26]. Overexpression of NL2 selectively causes a moderate increase in inhibitory synapses and enhances inhibitory synaptic function in cultured hippocampal neurons [27]. Based on our immunofluorescence staining combined with electrophysiological experiments, we speculate that NL2 alleviated bone cancer-induced pain by decreasing the activity of glutamatergic neurons, which directly reduced interneuronal excitability. In summary, our data strongly implicate NL2 in the regulation of inhibitory synaptic transmission of glutamatergic interneurons in BCP.

Accumulating evidence associates *NL3* mutations with autism [28]. It has been reported that pain is strongly correlated with the development of depression [29, 30], and mental and psychological disorders are in turn associated with autism [31]. In our experiments, NL3 was found to be decreased in the spinal cords of carcinoma-bearing rats. However, overexpression of NL3 in the spinal dorsal horn did not alleviate the hyperalgesia of BCP rats, suggesting that NL3 is not involved in BCP. The underlying mechanism causing NL3 to be decreased in BCP rats needs further investigation.

5. Conclusions

Our study identified a novel mechanism of bone cancer-induced pain regulated by NL1 and NL2 in spinal cord. In rats with carcinoma inoculation, NL1 and NL2 may reduce the excitability of GABAergic interneurons and the release of inhibitory synaptic neurotransmitters by glutamatergic interneurons, respectively, which affects the balance of the excitatory and inhibitory potential of interneurons and may cause the hyperalgesia of carcinoma-bearing rats. These results provide novel insights into the onset and progression of BCP.

List Of Abbreviations

AMPAR, α-amino-3-hydroxy-5-methyl-4-isoxazole propionic acid receptor; AP, action potential; BCP, bone cancer pain; ChE, cholinesterase-homology; DRG, dorsal root ganglion; EGTA, ethylene glycol-bis(b-aminoethyl ether)-N,N,N′,N′-tetraacetic acid; GABA, γ-aminobutyric acid; GAD, glutamic acid decarboxylase; gcGFP, lentiviral vectors containing green fluorescent protein; GO, Gene Ontology; HEPES, 4-(2-hydroxyethyl)-1-piperazine-ethanesulfonic acid; LG, laminin G-like; NL, neuroligin; NRXN, neurexin;

PBS, phosphate-buffered saline; NMDAR, N-methyl-D-aspartate receptor; PSD-95, postsynaptic density protein-95; PWT, paw withdrawal threshold; qRT-PCR, quantitative real-time polymerase chain reaction; sEPSCs, spontaneous excitatory postsynaptic currents; sIPSCs, spontaneous inhibitory postsynaptic currents; sPSCs, spontaneous postsynaptic currents; vGlut2, vesicular glutamate transporter 2

Declarations

Ethics approval and consent to participate: All experimental procedures and protocols used in this study were approved by the Animal Use and Care Committee of Hubei University of Medicine (Hubei, China) and were conducted in accordance with the National Institutes of Health (NIH) guide for the care and use of laboratory animals and with the ethics guidelines of the International Association for the Study of Pain. The informed consent for study participation in the declaration section.

ARRIVE statement: The study is reported in accordance with ARRIVE guidelines.

Consent for publication: Not applicable.

Availability of data and materials:All data generated or analyzed during this study are included in this published article.

Competing interests: The authors declare that they have no competing interests.

Funding: This work was supported by the National Natural Science Foundation of China (*NO*. 81971060), the Natural Science Foundation of Hubei Province of China (*NO.* 2020CFB342), the Natural Science Foundation of Hubei Provincial Department of Education (*NO.* B2018116) and the Scientific and Technological Project of Shiyan City of Hubei Province (*NO*. 19Y39 and 19Y41).

Authors' contributions: Xianqiao Xie, Changbin Ke and Shanchun Su conceived of the study and participated in its design. Xiaohui Li, Xueqin Xu, Dongsheng Sun, Yan Gao,Yanqiong Wu and Minjing Peng established the animal model of bone cancer pain. Yang Li and Xianqiao Xie cultured the primary neurons and implemented the electrophysiology experiment. Xianqiao Xie performed the experiment of immunohistochemistry,PT-PCR and western blotting,and was a major contributor in writing the manuscript. All authors read and approved the final manuscript.

Acknowledgements: Not applicable.

References

1. Varoqueaux F, Aramuni G, Rawson R L, Mohrmann R, Missler M, Gottmann K, *et al.* Neuroligins determine synapse maturation and function. Neuron, 2006, 51(6): 741–754.
2. Baudouin S, Scheiffele P. SnapShot: Neuroligin-neurexin complexes. Cell, 2010, 141(5): 908, 908 e901.

3. Levinson J N, Li R, Kang R, Moukhles H, El-Husseini A, Bamji S X. Postsynaptic scaffolding molecules modulate the localization of neuroligins. Neuroscience, 2010, 165(3): 782–793.
4. Hoon M, Soykan T, Falkenburger B, Hammer M, Patrizi A, Schmidt K F, *et al.* Neuroligin-4 is localized to glycinergic postsynapses and regulates inhibition in the retina. Proc Natl Acad Sci U S A, 2011, 108(7): 3053–3058.
5. Tzer-Bin Lin C-Y L, Ming-Chun Hsieh, Jian-Lin Jiang. Student, Jen-Kun Cheng, Yat-Pang Chau, Ting Ruan, Gin-Den Chen, Hsien-Yu Peng. Neuropathic Allodynia Involves Spinal Neurexin-1β-dependent Neuroligin-1/Postsynaptic Density-95/NR2B Cascade in Rats. Anesthesiology, 2015, 123(4): 909–226.
6. Mondin M, Labrousse V, Hosy E, Heine M, Tessier B, Levet F, *et al.* Neurexin-neuroligin adhesions capture surface-diffusing AMPA receptors through PSD-95 scaffolds. J Neurosci, 2011, 31(38): 13500–13515.
7. Budreck E C, Kwon O B, Jung J H, Baudouin S, Thommen A, Kim H S, *et al.* Neuroligin-1 controls synaptic abundance of NMDA-type glutamate receptors through extracellular coupling. Proc Natl Acad Sci U S A, 2013, 110(2): 725–730.
8. Choii G, Ko J. Gephyrin: a central GABAergic synapse organizer. Exp Mol Med, 2015, 47: e158.
9. Antonelli R, Pizzarelli R, Pedroni A, Fritschy J M, Del Sal G, Cherubini E, *et al.* Pin1-dependent signalling negatively affects GABAergic transmission by modulating neuroligin2/gephyrin interaction. Nat Commun, 2014, 5: 5066.
10. Shipman S L, Schnell E, Hirai T, Chen B S, Roche K W, Nicoll R A. Functional dependence of neuroligin on a new non-PDZ intracellular domain. Nat Neurosci, 2011, 14(6): 718–726.
11. Marro S G, Chanda S, Yang N, Janas J A, Valperga G, Trotter J, *et al.* Neuroligin-4 Regulates Excitatory Synaptic Transmission in Human Neurons. Neuron, 2019, 103(4): 617-626 e616.
12. Guo R, Li H, Li X, Sun Y, Miao H, Ma D, *et al.* Increased Neuroligin 2 Levels in the Postsynaptic Membrane in Spinal Dorsal Horn may Contribute to Postoperative Pain. Neuroscience, 2018, 382: 14–22.
13. Dolique T, Favereaux A, Roca-Lapirot O, Roques V, Leger C, Landry M, *et al.* Unexpected association of the "inhibitory" neuroligin 2 with excitatory PSD95 in neuropathic pain. Pain, 2013, 154(11): 2529–2546.
14. Zhao J Y, Duan X L, Yang L, Liu J P, He Y T, Guo Z, *et al.* Activity-dependent Synaptic Recruitment of Neuroligin 1 in Spinal Dorsal Horn Contributed to Inflammatory Pain. Neuroscience, 2018, 388: 1–10.
15. Spicarova D, Adamek P, Kalynovska N, Mrozkova P, Palecek J. TRPV1 receptor inhibition decreases CCL2-induced hyperalgesia. Neuropharmacology, 2014, 81: 75–84.
16. Yao W, Zhao H, Shi R, Li X, Li Y, Ke C, *et al.* Recombinant protein transduction domain-Cu/Zn superoxide dismutase alleviates bone cancer pain via peroxiredoxin 4 modulation and antioxidation. Biochemical and Biophysical Research Communications, 2017, 486(4): 1143–1148.
17. Ashburner M, Ball C A, Blake J A, Botstein D, Butler H, Cherry J M, *et al.* Gene ontology: tool for the unification of biology. The Gene Ontology Consortium. Nat Genet, 2000, 25(1): 25–29.

18. Jedlicka P, Vnencak M, Krueger D D, Jungenitz T, Brose N, Schwarzacher S W. Neuroligin-1 regulates excitatory synaptic transmission, LTP and EPSP-spike coupling in the dentate gyrus in vivo. Brain Struct Funct, 2015, 220(1): 47–58.
19. Ke C, Gao F, Tian X, Li C, Shi D, He W, *et al.* Slit2/Robo1 Mediation of Synaptic Plasticity Contributes to Bone Cancer Pain. Mol Neurobiol, 2017, 54(1): 295–307.
20. Espinosa F, Xuan Z, Liu S, Powell C M. Neuroligin 1 modulates striatal glutamatergic neurotransmission in a pathway and NMDAR subunit-specific manner. Front Synaptic Neurosci, 2015, 7: 11.
21. Shipman S L, Nicoll R A. A subtype-specific function for the extracellular domain of neuroligin 1 in hippocampal LTP. Neuron, 2012, 76(2): 309–316.
22. Chih B, Engelman H, Scheiffele P. Control of excitatory and inhibitory synapse formation by neuroligins. Science, 2005, 307(5713): 1324–1328.
23. Dahlhaus R, Hines R M, Eadie B D, Kannangara T S, Hines D J, Brown C E, *et al.* Overexpression of the cell adhesion protein neuroligin-1 induces learning deficits and impairs synaptic plasticity by altering the ratio of excitation to inhibition in the hippocampus. Hippocampus, 2010, 20(2): 305–322.
24. Li J, Han W, Pelkey K A, Duan J, Mao X, Wang Y X, *et al.* Molecular Dissection of Neuroligin 2 and Slitrk3 Reveals an Essential Framework for GABAergic Synapse Development. Neuron, 2017, 96(4): 808-826 e808.
25. Gibson J R, Huber K M, Sudhof T C. Neuroligin-2 deletion selectively decreases inhibitory synaptic transmission originating from fast-spiking but not from somatostatin-positive interneurons. J Neurosci, 2009, 29(44): 13883–13897.
26. Xia Q Q, Xu J, Liao T L, Yu J, Shi L, Xia J, *et al.* Neuroligins Differentially Mediate Subtype-Specific Synapse Formation in Pyramidal Neurons and Interneurons. Neurosci Bull, 2019, 35(3): 497–506.
27. Chubykin A A, Atasoy D, Etherton M R, Brose N, Kavalali E T, Gibson J R, *et al.* Activity-dependent validation of excitatory versus inhibitory synapses by neuroligin-1 versus neuroligin-2. Neuron, 2007, 54(6): 919–931.
28. Ravyts S G, Dzierzewski J M, Grah S C, Buman M P, Aiken-Morgan A T, Giacobb P R, Jr., *et al.* Pain inconsistency and sleep in mid to late-life: the role of depression. Aging Ment Health, 2019, 23(9): 1174–1179.
29. Nicholas M K. Depression in people with pain: There is still work to do Commentary on 'Understanding the link between depression and pain'. Scand J Pain, 2011, 2(2): 45–46.
30. Nicholas M K. Understanding the link between depression and pain. Scand J Pain, 2011, 2(2): 45–46.
31. Mohammad Ghaziuddin N G, And John Greden. Depression in Persons with Autism: Implications for Research and Clinical Care. Journal of Autism and Developmental Disorders, 2002, 32(4): 299–306.

Figures

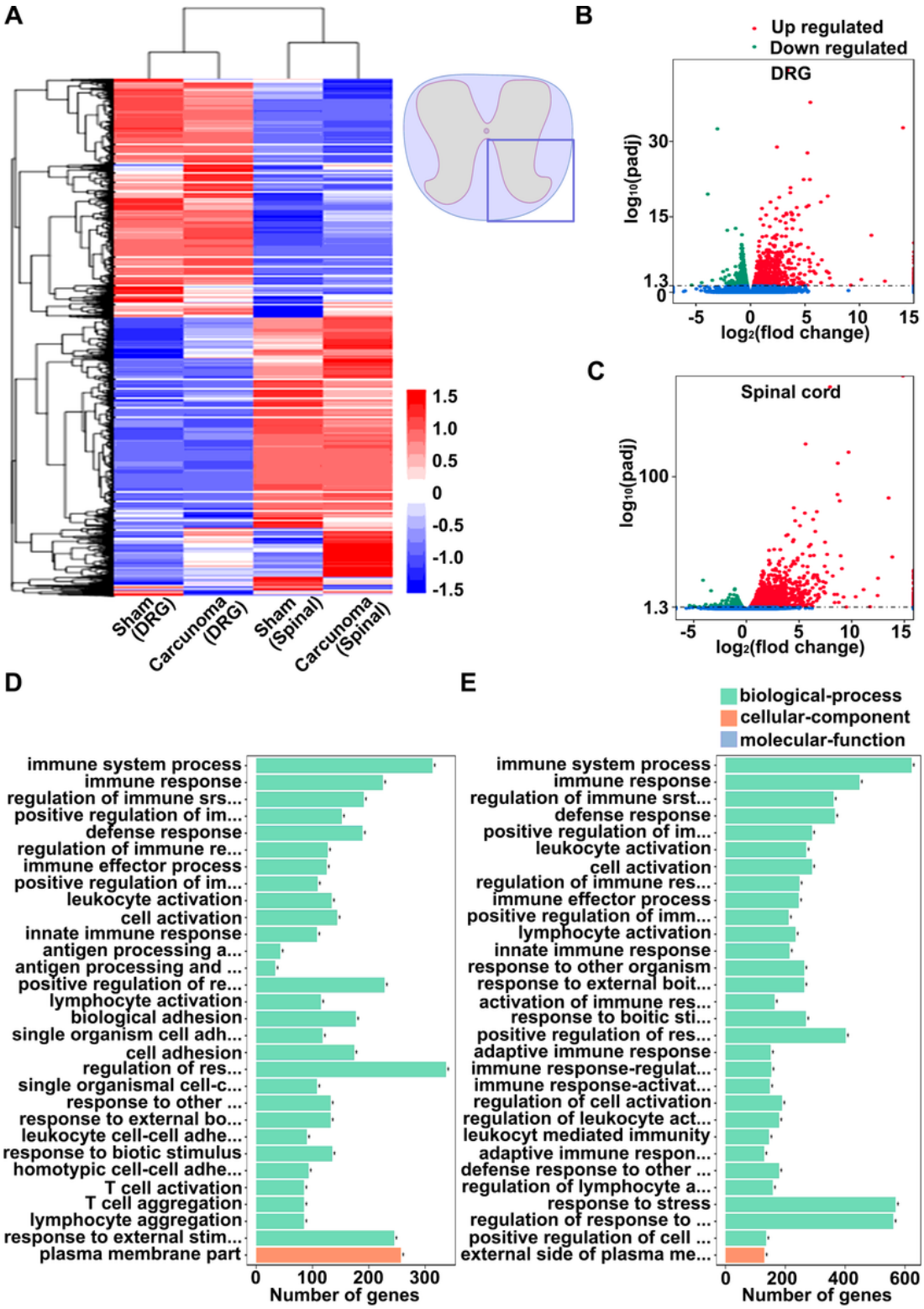

Figure 1

Illumina HiSeqTM analysis reveals pain-related genes in spinal dorsal horn and dorsal root ganglia of carcinoma-bearing rats. A. Cluster heat map of differentially expressed genes in spinal dorsal horn and dorsal root ganglia (DRGs) of carcinoma-bearing rats and sham controls. Expression values are scaled by rows with values greater than the mean displayed in red and those smaller than the mean in blue, and the intensity of color corresponding to the relative level of expression. Top right: illustration of the harvested

spinal cord and DRGs from carcinoma-bearing rats and sham controls. B, C. Volcano plot of differentially expressed genes in DRGs (B) and spinal dorsal horn (C) in carcinoma-bearing rats compared with sham controls. The red spots represent significantly upregulated genes, the green ones significantly downregulated genes, and the blue spots indicate unaltered genes. D, E. Gene Ontology analysis indicating enrichment of differentially expressed genes according to biological processes in DRGs (D) and spinal dorsal horn (E) of carcinoma-bearing rats versus sham controls.

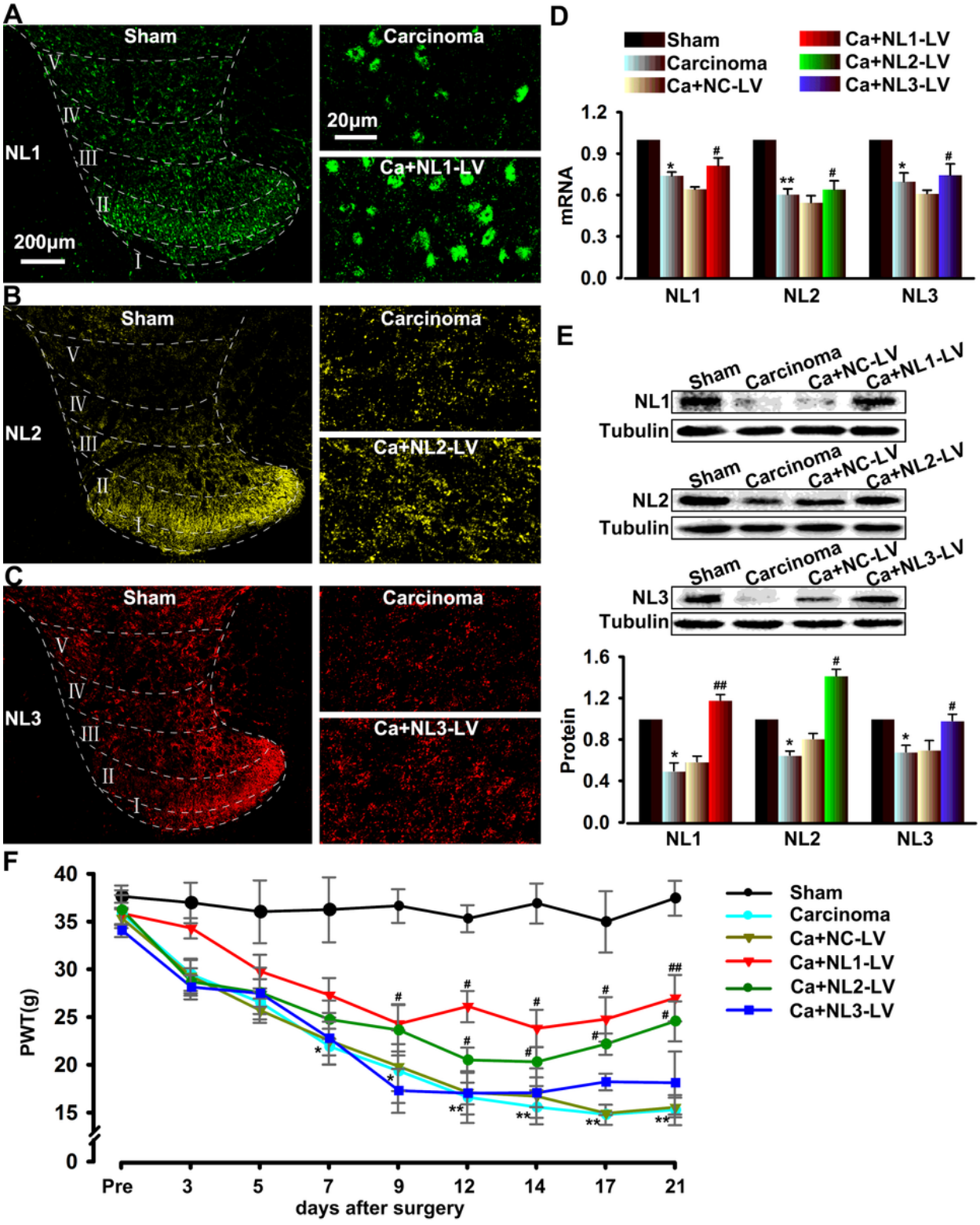

Figure 2

Diminished expression of NL1 and NL2 is associated with bone cancer pain. A–C. Immunofluorescent labeling of NL1 (green), NL2 (yellow), and NL3 (red) in the spinal dorsal horn of sham and cancer-bearing rats with lentivirus-mediated NL1 overexpression (A), NL2 (B), and NL3 (C). D, E. Quantitative analysis of NL1, NL2, and NL3 using RT-PCR (D) and Western blot analysis (E) of spinal cord. Values represent the mean ± SEM, n = 4. *P < 0.05. F. Mechanical allodynia was measured by paw withdrawal threshold (PWT). *P < 0.05 compared with sham rats, **P < 0.01; #P < 0.05 compared with carcinoma + NC-LV group, ##P < 0.01; n = 12 rats/group. All data are mean ± SEM.

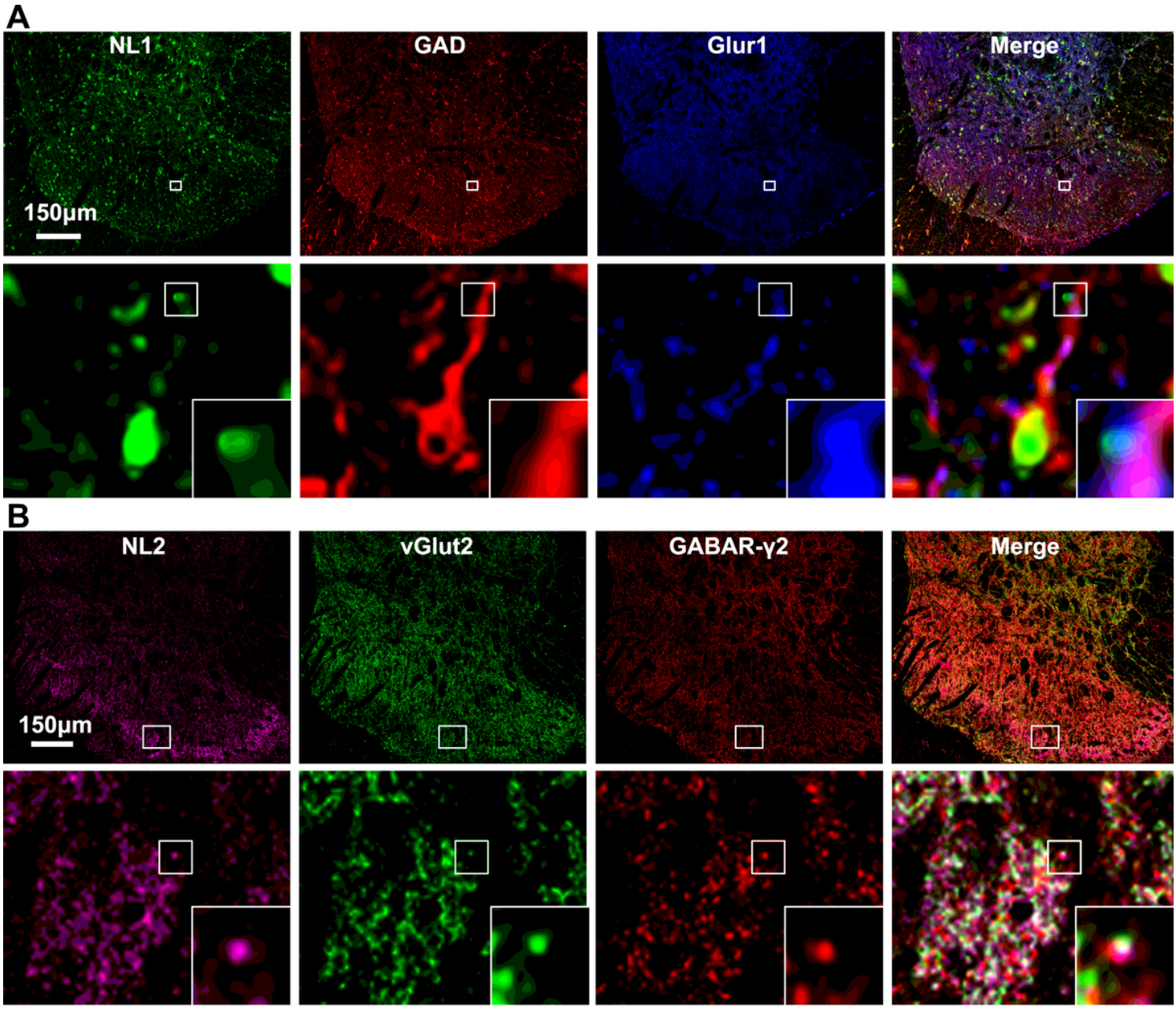

Figure 3

NL1 and NL2 are localized at GABAergic and glutamatergic neurons, respectively, in the spinal cord of rats. A. Multiple immunostainings showing that NL1 (green) co-localized with glutamic acid decarboxylase (GAD; red) and glutamate receptor 1 (blue) in the spinal dorsal horn. Magnified images (bottom) depicting that NL1 was localized on excitatory synapses of GAD-positive neurons. Scale bar =

150 μm. B. Immunofluorescence images showing that NL2 (magenta) co-localized with vesicular glutamate transporter 2 (vGlut2; green) and γ-aminobutyric acid receptor-γ2 (GABAR-γ2; red) in the spinal dorsal horn. Magnified images (bottom) indicating that NL2 was localized at inhibitory synapses in vGlut2-positive neurons. Scale bar = 150 μm.

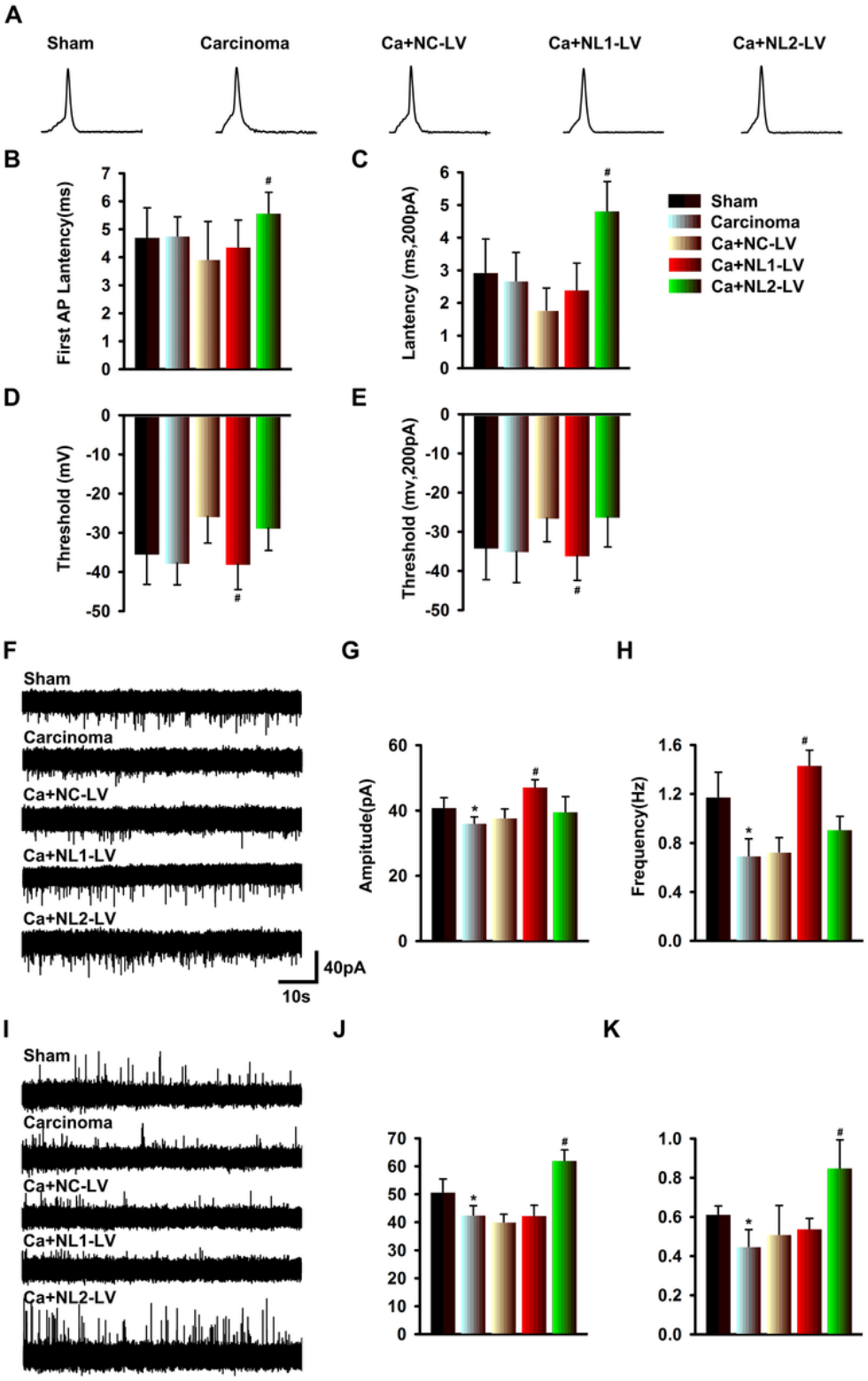

Figure 4

Electrophysiological properties of spinal cord interneurons expressing NL1 and NL2 in BCP rats. A. Representative traces of evoked action potentials (APs) in acute spinal slices of sham, carcinoma, carcinoma + NC-LV, carcinoma + NL1-LV, and carcinoma + NL2-LV rats. B, C. Overexpression of NL2 increased the latency of the first AP and that of the AP stimulated by 200 pA. D, E. NL1 overexpression decreased the threshold of the first AP and that of the AP stimulated by 200 pA. F. Traces of spontaneous EPSCs of acute spinal slices of sham, carcinoma, carcinoma + NC-LV, carcinoma + NL1-LV, and carcinoma + NL2-LV rats. G, H. Frequency (G) and amplitude (H) of spontaneous EPSCs (n = 46 for sham, n = 23 for carcinoma, n = 7 for carcinoma + NC-LV, n = 32 for carcinoma + NL1-LV, and n = 7 for carcinoma + NL2-LV; *P < 0.05 compared with sham; #P < 0.05 compared with carcinoma + NC-LV group.). I. Traces of spontaneous IPSCs of acute spinal slices of sham, carcinoma, carcinoma + NC-LV, carcinoma + NL1-LV, and carcinoma + NL2-LV rats. J, K. Frequency (G) and amplitude (H) of spontaneous IPSCs (n = 46 for sham, n = 23 for carcinoma, n = 7 for carcinoma + NC-LV, n = 32 for carcinoma + NL1-LV, and n = 7 for carcinoma + NL2-LV; *P < 0.05 compared with sham; #P < 0.05 compared with carcinoma + NC-LV group).

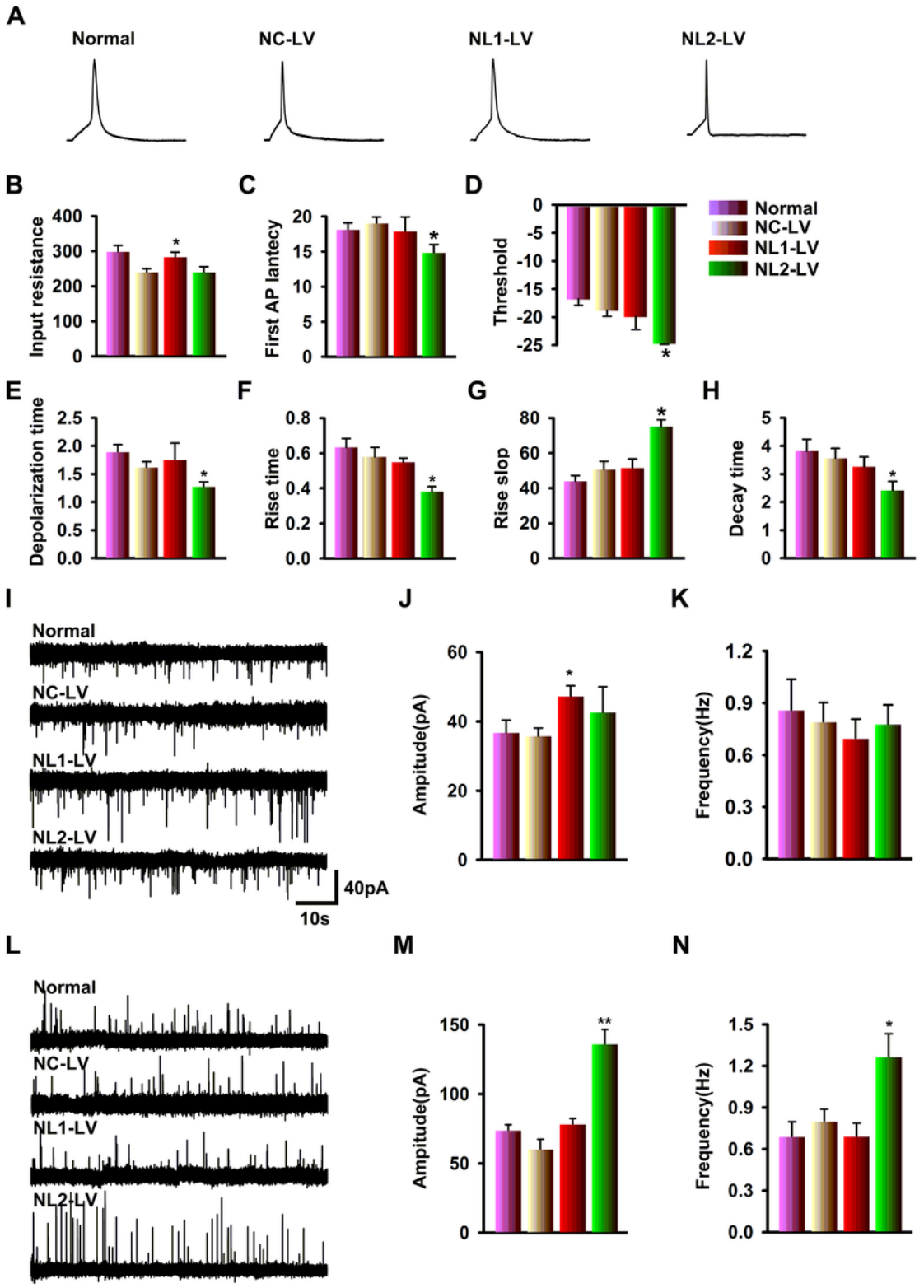

Figure 5

Electrophysiological properties of primary cultured rat cortical neurons with NL1 or NL2 overexpression. A. Representative traces of evoked APs of untransfected, NC-LV, NL1-LV, or NL2-LV transfected cortical neurons of neonatal rats. B. NL1 overexpression increased the input resistance of neurons compared with those transfected with NC-LV (n = 32 for untransfected, n = 39 for NC-LV, and n = 26 for NL1-LV; *P < 0.05 compared with NC-LV). C–H. Overexpression of NL2 decreased the latency, rise time, and decay time, and

increased the rise slope of the first AP. NL2 overexpression decreased the depolarization time and increased the threshold of APs evoked by a current of 200 pA compared to neurons transfected with NC-LV (n = 32 for untransfected, n = 39 for NC-LV, and n = 17 for NL2-LV; *P < 0.05 compared with NC-LV). I. Traces of spontaneous EPSCs of untransfected, NC-LV, NL1-LV, or NL2-LV transfected cortical neurons. J, K. Frequency (J) and amplitude (K) of spontaneous EPSCs (n = 13 for untransfected, n = 31 for NC-LV, n = 30 for NL1-LV, and n = 25 for NL2-LV; *P < 0.05 compared with NC-LV). L. Traces of spontaneous IPSCs of untransfected, NC-LV, NL1-LV, or NL2-LV transfected cortical neurons. M, N. Frequency (J) and amplitude (K) of spontaneous IPSCs (n = 13 for untransfected, n = 27 for NC-LV, n = 33 for NL1-LV, and n = 25 for NL2-LV; *P < 0.05 compared with NC-LV).

Supplementary Files

This is a list of supplementary files associated with this preprint. Click to download.

- Supplementaldate.docx